HHS Public Access

Author manuscript

Adv Funct Mater. Author manuscript; available in PMC 2024 February 23.

Published in final edited form as:

Adv Funct Mater. 2023 February 23; 33(9): . doi:10.1002/adfm.202207388.

Deep Eutectic Solvents-based Ionogels with Ultrafast Gelation and High Adhesion in Harsh Environments

Gang Ge[1,2], **Kalpana Mandal**[1], **Reihaneh Haghniaz**[1], **Mengchen Li**[3], **Xiao Xiao**[2], **Larry Carlson**[4], **Vadim Jucaud**[1,*], **Mehmet Remzi Dokmeci**[1,*], **Ghim Wei Ho**[2,*], **Ali Khademhosseini**[1,*]

[1]Terasaki Institute for Biomedical Innovation, Los Angeles, CA, USA

[2]Department of Electrical and Computer Engineering, National University of Singapore, 4 Engineering Drive 3, Singapore 117583, Singapore

[3]Department of Materials Science & Engineering, University of California-Los Angeles, Los Angeles, CA, USA

[4]Institute for Technology Advancement, University of California-Los Angeles, Los Angeles, CA, USA

Abstract

Adhesive materials have recently drawn intensive attention due to their excellent sealing ability, thereby stimulating advances in materials science and industrial usage. However, reported adhesives usually exhibit weak adhesion strength, require high pressure for strong bonding, and display severe adhesion deterioration in various harsh environments. In this work, instead of water or organic solvents, a deep eutectic solution (DES) was used as the medium for photopolymerization of zwitterionic and polarized monomers, thus generating a novel ionogel with tunable mechanical properties. Multiple hydrogen bonds and electrostatic interactions between DES and monomers facilitated ultrafast gelation and instant bonding without any external pressure, which was rarely reported previously. Furthermore, high adhesion in different harsh environments (e.g., water, acidic and basic buffers, and saline solutions) and onto hydrophilic (e.g., glass and tissues) and hydrophobic (e.g., polymethyl methacrylate, polystyrene, and polypropylene) adherends was demonstrated. Also, high stretchability of the ionogel at extreme temperatures (−80 and 80 °C) indicated its widespread applications. Furthermore, the biocompatible ionogel showed high burst pressure onto stomach and intestine tissues to prevent liquid leakage, highlighting its potential as an adhesive patch. This ionogel provides unprecedented opportunities in the fields of packaging industry, marine engineering, medical adhesives, and electronic assembly.

Graphical Abstract

* vjucaud@terasaki.org; mdokmeci@terasaki.org; khademh@terasaki.org; elehgw@nus.edu.sg.

Conflict of Interest

The authors declare no conflicts between author contributions and financial interest.

Supporting Information

The Supporting Information is available from the Wiley Online Library.

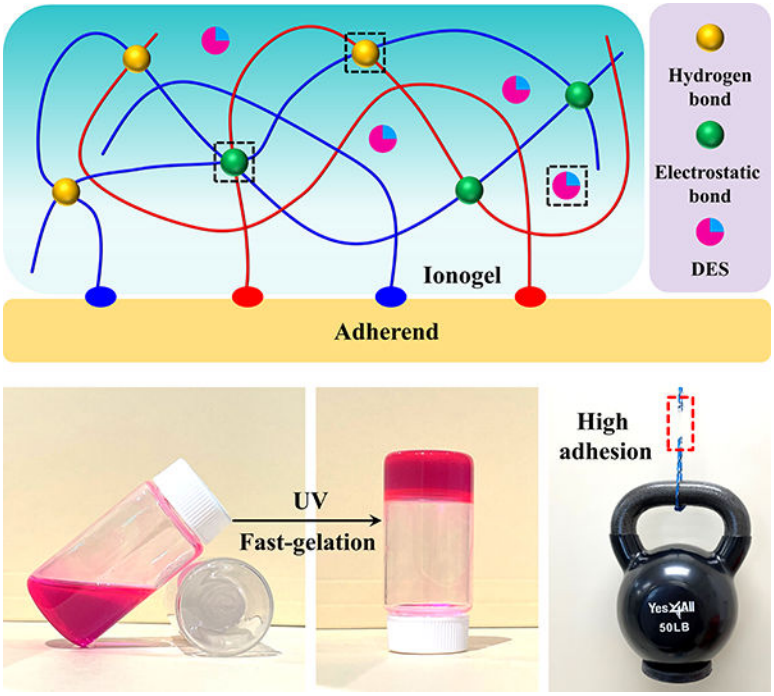

By utilizing deep eutectic solvents as a green media for the photopolymerization of zwitterionic and polarized monomers, a novel ionogel with ultrafast gelation and instant bonding properties is proposed. Strong adhesion in harsh environments (*e.g.*, underwater, acidic and basic buffers, and saline solutions), ductile stretchability, high biocompatibility, and desirable burst pressure highlight the ionogel's widespread applications.

Keywords

Ionogel; deep eutectic solvent; fast gelation; strong adhesion; harsh environments

1. Introduction

Adhesives are defined as a class of sticky, soft materials with strong adhesion to adherends, [1] and they have a great potential in automobile assembly,[2] packaging industry,[3] human-machine interfaces,[4] and flexible electronics.[5, 6] Adhesives include two subsets: water- (e.g., hydrogel adhesives) and solvent-based (e.g., ionogel adhesives) species. [7] Hydrogel adhesives based on catechol-containing derivative,[8] metal-coordination, [9] cationic-aromatic sequence,[10] and carboxyl-amino chemistry[11] usually show low adhesion strengths (28 to 60 kPa). Furthermore, these motifs are subject to redox-, pH-, and ion-initiated debonding.[12] Another drawback of hydrogel adhesives is that tedious procedures for topological crosslinking, including plasma treatment, siloxane chemistry, and hydrolysis,[13, 14] should be implemented, which drastically change near-surface and internal properties of the adherend. Moreover, hydrogel adhesives are vulnerable to hydrolytic degradation, plasticization, and solvation[15] since free water within hydrogel networks dilutes the interfacial bonding density and obstructs direct contact between the adhesive

and adherend.[16] For example, Yang et al. has demonstrated the complete detachment of poly(2-hydroxyethyl methacrylate) superglues from glass adherends within 170 s after adding water[17] because conformation rearrangements and coacervation variations of the polymers disrupted non-covalent interactions.[18] To relieve the poor adhesion of adhesives induced by water, researchers turned to adopting organic solvents as media of adhesives.[19, 20] However, such volatile organic compounds (VOCs), including dimethyl sulphoxide,[19] cyanoacrylate derivatives,[21] and acetonitrile,[20] released cytotoxic ingredients during degradation.[22] Lee et al. demonstrated that commercial poly(vinyl chloride) and 3M epoxy adhesives released smelly VOCs, which caused pulmonary inflammation and fibrosis in mice.[23] Besides, these adhesives only worked for dry adherends under ambient temperatures, largely limiting the potential usage. Therefore, developing new green solvent media-based novel adhesives, which retain high adhesion in various harsh environments (e.g., water, non-neutral buffers, and saline solvents), is highly needed. Besides, the adhesives should show low toxicity and high biocompatibility to reduce health risk, broad working windows (e.g., subzero and high temperatures), and ubiquitous adhesion onto various adherends (e.g., hydrophilic/hydrophobic adherends and even brimming surfaces).

Instead of water or organic solvents, ionic liquids (ILs) have been recently used to develop strong ionogel adhesives with enhanced interfacial bonding due to variable ion pairs in ILs, which dynamically interacted with polymer chains.[24, 25] Nevertheless, high external pressure was usually required for successful bonding.[26] Yan et al. proposed one ionogel with a satisfactory adhesion strength (5.8 MPa) by utilizing the ILs as media; however, an ultra-high loading (40 kPa) was needed to form the bonding layer, which could result in permanent damage to the adherent.[27] Besides, formed crystals within ionogels indicated unstable adhesion at different temperatures.[26, 27] Ionogels based on fluorine-rich ILs exhibited underwater adhesion only after being formulated into stretchable bulks, hindering their possibilities as superglues.[28, 29] Furthermore, the adhesion strength (681 kPa) was insufficient to stick distinct materials together.[28] More recently, deep eutectic solvents (DESs), sharing similar properties with ILs, were introduced to improve adhesion strengths (6.8 MPa) due to the multiple supramolecular interactions.[30] However, long-term pressing (10 mins) was required, which was inadequate for many rapid interventions such as first-aid emergencies. Generally, rapidly gelled adhesives showed decreased adhesion since polymer chains with unoptimized conformations do not effectively diffuse and penetrate into adherends in a short time.[31] The adhesive with fast gelation (28 s) demonstrated a low interfacial strength of 6.8 kPa.[32] Therefore, mechanically strong and sticky adhesives with high adhesion and ultrafast gelation are warranted. Novel synthesis approaches should potentially utilize new chemicals (i.e., monomers and solution media) while optimizing intermolecular interactions between both.[30, 32]

In this paper, we report a mechanically strong ionogel prepared by photopolymerization of polarized N-hydroxyethyl acrylamide (HEAA) and zwitterionic N-(3-sulfopropyl)-N-(methacryloxyethyl)-N, N-dimethylammonium betaine (DMAPS) in DESs, a type of water-free green solvent. Fast gelation was achieved on account of multiple intra- and intermolecular interactions among different components. Mechanical and electrochemical properties of ionogels were shown to be tunable by changing the formulations. We demonstrated that instant and strong bonding of ionogels onto hydrophobic adherends under

harsh environments (e.g., water, acidic and basic buffers, saline solutions, and brimming surfaces) was obtained without the use of external pressure. High stretchability at extreme temperatures (−80 and 80 °C) also indicated the feasibility of using these ionogels for broad applications. Furthermore, the biocompatible ionogels survived high burst pressure and prevented liquid leakage after sealing punctured stomach and intestine tissues. Fast gelation, strong adhesion, and high biocompatibility displayed the ionogel's potential applications for the medical adhesives, marine engineering, as well as electronic assembly.

2. Results and Discussion

2.1 Structural Design and Fast Gelation of the Ionogels

The water-free ionogel containing poly(N-hydroxyethyl acrylamide) (PHEAA) and poly(N-(3-sulfopropyl)-N-(methacryloxyethyl)-N, N-dimethylammonium betaine) (PDMAPS) was prepared by the one-step co-polymerization of their corresponding monomers (Figure 1a). Co-polymerization together with crosslinking occurred at the same time in DESs.[33] As one kind of green solvent comparable to ILs,[34] DES was used as the precursor media to facilitate performance tuning. Indeed, the hydrogen bonds within DES can be readily tuned based on the donor/acceptor categories and their molar ratios.[35] In this system, the transparent and viscous DES was prepared by mixing choline chloride (ChCl) and glycerol, which served as a hydrogen bond acceptor and donor, respectively.[35] The electrostatic interactions of the N^+-Cl^- bonds enhanced the ionic features of DES.[35, 36] Polarized PHEAA, which has excellent resistance to both water and corrosion, was chosen to construct the first crosslinked network. Zwitterionic PDMAPS was added to enhance the durability underwater of the ionogel since the co-presence of anions and cations facilitated the formulation of a hydration shell without sacrificing hydrogen bonds.[37] Besides, multiple electrostatic interactions between DES and PDMAPS also enhanced the adhesion feature underwater.[11]

D_xH_y denotes specific ionogel formulations, where x:y refers to the volume ratios of DES and HEAA. Multiple dynamic intra- and intermolecular interactions within different components were present in the proposed ionogel. In detail, hydroxy and amino groups of PHEAA effectively formed intra- and intermolecular hydrogen bonds. Hydroxy and amino groups of PHEAA, hydroxy groups of glycerol, and hydroxy groups of ChCl interacted with each other. This interaction enhanced the mechanical performances of the ionogel through hierarchical hydrogen bonding. Oxygen anions (O^-) in PDMAPS and chloride anions (Cl^-) in ChCl formed electrostatic interactions with quaternary ammonium cations (N^+) of PDMAPS and ChCl, respectively. Moreover, the N^+ cations combined with adjacent ions benefit delocalization of electrons and rigidness of polymer configurations, favoring a topological ionic matrix of the ionogel.[38] Zeta potential showed that the DES was negatively charged (−41.83 mV), however, it became almost neutral (0.3 mV) after adding HEAA (Figure S1a). The further addition of DMAPS resulted in the precursor with positive charge (1.9 mV). Such charge variations were because of the multiple intermolecular interactions between different components, confirmed by the Fourier Transform Infrared Spectroscopy (FTIR) (Figure S1b).

Confocal laser scanning microscopy (CLSM) demonstrated the structural evolution of the ionogel after different UV exposure times (from 0 to 120 s) (Figure 1b). Initially, the surface of the liquid precursor was smooth and flat before UV exposure. However, upon UV exposure for 60, 80, and 120 s, the ionogel showed an incrementally aligned profile. Possibly, the highly ordered structure resulted from the interfacial self-assembly of networks during polymerization.[39] The stained liquid precursor was rapidly converted into a gel after UV exposure. Although the gelation time varied between formulations, all ionogels demonstrated a fast gelation capacity (Figure 1c). Both storage modulus (G') and loss modulus (G") of the D_1H_4 ionogel reached a steady platform upon UV exposure for 36 s, and a much larger G' value demonstrated the gel state (Figure 1d). After gelation, the D_3H_2 ionogel showed high adhesion onto the measuring plate of the rheometer when the plate was lifted (Figure S2). Overall, the ratios between DES and HEAA significantly influenced the gelation time of the ionogel, from 14 s for D_4H_1 to 36 s for D_1H_4 (Figure 1e and S3). For example, the D_2H_3 ionogel gelled in 28 s (G' = 100.4 kPa and G" = 66.5 kPa). With more DES, D_3H_2 and D_4H_1 formed the bulk ionogel after UV exposure for 21 and 14 s, respectively. In contrast, after UV exposure for 2 mins, precursors without DMAPS or HEAA exhibited a higher G" than G', indicating that no gelation occurred (Figure S4). A recent study demonstrated that the increased concentration of DES favored fast gelation compared to water[33] because the DES could significantly enhance the overall polymerization rate in the eutectic media via the multiple hydrogen and ionic bonds. Therefore, more DES largely accelerated the polymerization process, resulting in quicker gelation. Such polymerization-induced gelation was the synergy of chemical crosslinking and dynamic bonding. Since DES favors more dynamic interactions through non-covalent bonds, whereas HEAA enhances rigidity through covalent bonding, higher ratios of DES to HEAA were associated with softer and more flexible ionogels (Figure S5). Similarly, complex viscosity, which was an indicator of intermolecular interactions due to intrinsic friction, also showed a decreased trend upon adding more DES (Figure S6). Lastly, the D_4H_1 ionogel showed the least shear-thinning property because its networks were more dynamic to maintain the initial state (Figure S7).

2.2 Mechanical, Electrochemical, and Rheological Properties of the Ionogels

Recently reported strong glues exhibited high adhesion, but few demonstrated high stretchability because of irreversible covalent bonds. Since DES largely increases the softness of the crosslinked networks by providing an additional degree of freedom of polymer configurations, the coiled polymer chains can be easily unwrapped during stretching. Therefore, our ionogel demonstrated impressive mechanical compliance. Individual ionogel dots could be seamlessly solidified onto an ionogel film. Furthermore, the dotted ionogel could be biaxially stretched without any delamination, indicating high adhesion of the ionogel to itself (Figure 2a). Furthermore, ratios between DES and HEAA influenced stress-strain performances of the ionogel (Figure 2b). For example, the D_1H_4 ionogel could be stretched to 553% with a fracture strength of 441 kPa, sharing similar mechanical features to elastomers.[40] The D_2H_3 ionogel showed a higher stretchability of 743% and a lower fracture strength of 208 kPa. With more DES, the fracture strength of the D_3H_2 ionogel was further decreased to 111 kPa with a stretchability of 1235%. Compared with the polyacrylamide- and poly(acrylic acid)-based hydrogels, which could be stretched

500% and 1503%, respectively,[31, 41] the D_4H_1 ionogel showed a higher stretchability of 1942%, demonstrating its enhanced mechanical compliance. Young's modulus of the D_1H_4, D_2H_3, D_3H_2, and D_4H_1 ionogel were 327, 106, 29, and 0.75 kPa, respectively, indicating enhanced rigidity upon more HEAA. Note that J-shaped profiles of the D_1H_4, D_2H_3, and D_3H_2 ionogels became more obvious after increasing the amount of HEAA, which indicated the strain-stiffening behavior.[28] By comparison, the D_4H_1 ionogels showed the strain-softening properties due to the presence of increased non-covalent bonds. Indeed, adding more DES increased the softness and flexibility of the ionogel since DES favored more dynamic interactions through hydrogen bonds. Besides, both rigidity and fracture strength increased upon more photoinitiator and DMAPS contents (Figure S8). The dotted ionogel firmly adhered to the nitrile glove and curved surface (Figure S9), and was uniaxially stretched to 200% without breakage and delamination (Figure S10), further demonstrating high flexibility and strong adhesion. The ionogel was deposited onto an aluminum foil to assess its impedance (Figure 2c). The D_1H_4 ionogel showed the highest impedance in frequencies from 10^{-2} to 10^5 Hz. By comparison, the D_2H_3 ionogel showed a two-thirds lower impedance in the high-frequency range and nearly thirty-fold lower impedance in the low-frequency range. The D_3H_2 ionogel showed a hundred-fold lower impedance in the low-frequency range than the D_1H_4 ionogel. The D_4H_1 ionogel exhibited the lowest impedance. Under the external electrical field, N^+ cations shifted towards the cathode, whereas Cl^- anions migrated to the anode due to the potential difference.[15] Such directional ion migration resulted in the formation of conductive pathways.[35, 36] Because more DES and less polymer contents favored a higher ion concentration and lower migration barrier, the D_4H_1 ionogel with the most mobile ions and the sparsest crosslinked networks exhibited the highest ionic conductivity.

Frequency-dependent rheological tests were conducted to characterize the intermolecular interactions among different ionogel compositions (Figure 2d). Below a frequency of 1.8 Hz, D_1H_4 and D_2H_3 ionogels exhibited a gel state, but both transitioned to a liquid state at a frequency higher than 1.8 Hz. In comparison, the D_3H_2 and D_4H_1 ionogels did not exhibit a similar phase transition. Indeed, D_3H_2 and D_4H_1 ionogels remained in a constant gel state at both high and low frequencies because their networks exhibited more dynamic reversibility.[42] Moreover, at low frequency, the difference between G' and G" of the D_4H_1 ionogel was not as distinct as other ionogels, indicating intrinsic viscoelastic features of this formulation. As shown in Figure 2e, G' and G" of the D_1H_4 ionogel exhibited decreased profiles at a shear strain above 20.5%, indicating the irreversible feature of the crosslinked networks upon a high shear strain. However, the D_2H_3, D_3H_2, and D_4H_1 ionogels exhibited a steady platform from 0.01% to 100% shear strain ranges. Water-based hydrogel adhesives lost elasticity at subzero temperatures because the as-formed ice crystals hardened the hydrogel matrix.[43] In contrast, since DES was used as the medium instead of water, ionogels remained a gel state with a higher G' across broad temperature ranges (−20 to 100 °C) (Figure S11). Also, both G' and G" decreased with temperature due to the higher mobility of polymer segments.

Ionogels also demonstrated anti-freezing and heat-resistant capacities at both low (−80 °C) and high (80 °C) temperatures (Figure S12). The D_1H_4 ionogel stored at 80 °C for 1 h could be stretched to 480% with a fracture strength of 756 kPa. However, the D_1H_4 ionogel stored

at −80 °C showed a higher stretchability (703%) and a lower fracture strength (349 kPa) than the original one stored at 25 °C. The humidity-enhanced mechanical stretchability was attributed to the hygroscopicity of the DES and zwitterionic DMAPS.[36, 44] Since water can be volatile at room temperature (25 °C), traditional water-based hydrogels were limited to short-term usage (2 days).[45] In comparison, when DES was used as the media, these DES-based ionogels showed ductile compliance even after storage at room temperature for 15 days (Figure S13). Figure 2f depicted the influence of temperature on the viscosity of ionogels. The viscosity of the D_1H_4 ionogel decreased from 42.6 to 5.1 kPa, with the temperature increasing from −20 to 100 °C. The D_2H_3 ionogel exhibited a viscosity of 17.9 kPa at −20 °C and 2.9 kPa at 100 °C. At −20 °C, the viscosity of the D_3H_2 and D_4H_1 ionogels was 7.3 and 3.1 kPa, whereas it became 0.9 and 0.2 kPa at 100 °C, respectively. Indeed, the viscosity of the D_4H_1 ionogel was more influenced by temperature since more hydrogen bonds could be rearranged to retain the initial network configurations.

2.3 Adhesion Strength of Ionogels in Harsh Environments

Adhesive, cohesive, and structural failures are three main reasons for decreased adhesion, which is characterized by glue strength, strength between glue and adherends, and adherend strength, respectively (Figure 3a). Lap-shear tests were conducted to assess the adhesion capacity of ionogels onto adherends. In particular, the adhesion strength of the D_1H_4, D_2H_3, D_3H_2, and D_4H_1 ionogels was 0.97, 0.85, 0.43, and 0.12 MPa on polymethyl methacrylate (PMMA), and 0.81, 0.75, 0.41, and 0.02 MPa on polystyrene (PS), respectively (Figure 3b). By comparison, PMMA and PS sheets possessed a fracture strength of 4.9 and 1.3 MPa (Figure S14), much higher than the adhesion strength of ionogels onto adherends. Therefore, the adhesion failure of ionogels onto PMMA and PS adherends was mainly because of the adhesive and cohesive break. The D_1H_4 ionogel bonded PMMA exhibited a high adhesion strength and a low displacement, indicating the brittle failure (Figure S15). With more DES, displacements of the D_1H_4 ionogel bonded PMMA largely increased, which was in accordance with the ductile fracture. Optical images demonstrated that ionogels with more DES left more residue on the adherend surface (Figure S16). Microscopic images showed that the pure PMMA sheet possessed a smooth surface, whereas it became rough after the D_1H_4 ionogel was *in situ* gelled onto its surface (Figure S17). Such seamless contact between the D_1H_4 ionogel and the PMMA sheet favored high adhesion. Also, ionogels with more DES exhibited a curved surface onto the PMMA sheet, which accounted for less surface contact and reduced adhesion. Compared with water-based hydrogel adhesive, which failed under extreme temperatures due to easy water evaporation or freezing, this ionogel adhesive showed high adhesion under both high and subzero temperatures (Figure S18), indicating excellent tolerance. Adhesion strengths under 80 °C were slightly lower than those under −80 °C because high temperature increased chain mobility and viscosity (Figure S11).

The D_1H_4 ionogel possessed an excellent adhesion strength (7.8 MPa) on glass, much higher than other DES- and IL-based glues, whose adhesion strengths on glass were 5.8[27] and 6.8 MPa,[30] respectively (Figure S19a). In addition, the ionogel adhered between the copper sheet and PMMA showed higher adhesion strengths than those on the pure PMMA since metal coordinated with functional groups of polymers for enhanced molecular interactions

(Figure S19b).[43] One recent study demonstrated that the charged polymer-based hydrogels showed high adhesion by mimicking slug's defensive mucus.[11] Similarly, this charged zwitterions-based ionogels can form effective bonding sites with substrates. Besides, the interpenetrating networks can significantly dissipate the peeling energy through covalent bonds, hydrogen interactions, and electrostatic effects (Figure S1b).[11] Thus, both multiple molecular interactions and mechanical stretchability accounted for high adhesion of this ionogel.[1] Ionogels also showed long-term adhesion after storage at room temperature for 15 days (Figure 3c). The adhesion strength of the D_1H_4, D_2H_3, D_3H_2, and D_4H_1 ionogel onto PMMA was 1.04, 0.80, 0.29, and 0.005 MPa; and for PS, the adhesion strength was 0.78, 0.64, 0.16, and 0.004 MPa, respectively. Besides ambient conditions, the underwater environment also had a negligible influence on the high adhesion of the D_1H_4 ionogels onto an adherend (Figure 3d).

The ionogel fully swelled after underwater for 10 h and the adhesion strengths dramatically decreased (Figure S20), ascribing to the hygroscopicity of DES and PDMAPS without deteriorating hydrogen bonds.[37, 44] However, for *in vivo* applications, most adhesives are used on wet surfaces,[1] not underwater. Burst pressure is the more important parameter for adhesion on wet surfaces. Under such circumstances, our ionogel adhesive showed not only high adhesion on the wet tissue surface (Figure 5), but also the highest burst pressure (Table S1), compared with recently reported tissue adhesives. Therefore, these characteristics, together with its fast gelation, demonstrate that our ionogel is a competitive biomedical adhesive. The D_1H_4 ionogel bonded adherends exhibited a higher adhesion strength after being placed in acidic buffer solutions (Figure 3e). Indeed, the addition of acidic buffer promoted the delocalization of hydrogen donors to protonate anions and cations, facilitating multiple hydrogen bonds.[34, 46]

Besides, the D_1H_4 ionogel also exhibited a high adhesion strength in different saline solutions (Figure 3f). The D_1H_4 ionogel bonded PMMA showed adhesion strengths of 1.28, 1.12, and 1.30 MPa after storage in lithium chloride (LiCl), calcium chloride ($CaCl_2$), and magnesium chloride ($MgCl_2$) for 2 h, respectively. Adhesion strengths onto PS adherends were 1.05, 1.00, and 1.12 MPa for LiCl, $CaCl_2$, and $MgCl_2$ saline solutions, respectively. Saline solution affected the adhesion strength of ionogels through coordination interactions. Li^+ has the smallest cation radius, which favors strong ion-dipole interactions between Li^+ and functional groups (e.g., hydroxyl and amino groups) of the ionogel. Besides coordination interactions, the hydration effect was another significant factor influencing the underwater adhesion of adhesives. If saline ions bonded with more water to reduce its activity, then the water had less chance to contact adhesives directly.[15] LiCl, which displays high hydration enthalpy ($-520\ kJmol^{-1}$) and high solubility (> 13M),[47] could strongly bond water; therefore, solvents had a negligible influence on the adhesion. Mg^{2+} shares a similar bivalent charge as Ca^{2+}; however, the smaller ionic radius of Mg^{2+} indicated higher coordination interactions and lower water activity,[47] which contributed more to the adhesion strength of the ionogels. The D_1H_4 ionogel bonded PMMA could lift a 50 lbs kettlebell, and such high-weight bearing capacity was also retained after immersing the ionogel bonded PMMA in water for 2 h (Figure 3g). The highly adhesive D_1H_4 ionogel could also be used to bond several pieces of glass together and create a glass cup (Figure 3h). Even when the stained water was stored within the cup for 2 h, the cup retained

its original shape without water leakage. Together, these results provided possibilities for industrial packing and marine engineering applications.

2.4 *In Situ* Fast Gelation and High Adhesion of the Ionogels in Water and Acidic Solutions

Considering the high hygroscopicity of the DES and DMAPS, and multiple dynamic interactions within precursors, ionogels possessed *in situ* fast gelation underwater (Figure 4a). Initially, highly viscous liquid filaments were extruded into the water; however, a bulk of aggregated gel formed upon UV exposure (30 s), indicating fast gelation underwater. Water had almost no influence on the gelation dynamics of ionogels, thus confirming the fast sol-gel transformation process (Figure 4b and S21). Modulus of the ionogels gelled underwater also showed similar values to those gelled under ambient conditions (Figure 4c). Ionogels were also applied onto PMMA adherends in water and acidic solutions to assess their adhesive properties in harsh environments. Adhesion strengths of the D_1H_4 ionogel onto PMMA in water and acidic solutions were both 0.86 MPa, and these values for the D_2H_3, D_3H_2, and D_4H_1 ionogels were 0.57, 0.37, and 0.009 MPa, respectively (Figure 4d and 4e). There was no significant difference in adhesion strength compared to ionogels formed in ambient conditions. Both fast gelation capacity and multiple dynamic interactions of ionogels were responsible for the high adhesion strength in water and acidic solutions.

The comparison between the proposed ionogel and six recently developed adhesives was summarized in Figure 4f.[18, 48–52] Although the polyurethane adhesive showed high adhesion, high pressure (8 N cm^{-2}) and tedious processing procedures were required to form the bonding layer.[48] The photocurable catechol-grafted hyaluronic acid showed easy oxidation of catechol groups, resulting in decreased adhesion.[49] The hydrogel adhesives showed a lower adhesion (less than 300 kPa), thus limiting their usage scenarios.[18, 50, 51] The glue based on acidic ingredients, including poly(acrylic acid), polyvinylbenzenesulfonic acid, and poly(itaconic acid), faced possible acid leakage, resulting in adherends damage.[52] In contrast, the novel ionogel demonstrated fast gelation, strong adhesion strength under ambient and harsh conditions, and wide pH usage ranges. The ionogel could also be *in situ* gelled to prevent water leakage (Figure 4g). After UV exposure for 100 s, the D_1H_4 ionogel tightly bonded onto the polypropylene container surface to form the sealing layer. Even after storage under ambient conditions for 2 h, water height in the vessel did not show obvious variations, indicating strong and long-term adhesion of the ionogel in water.

2.5 Burst Pressure, *in vitro* Biocompatibility, and Adhesion of the Ionogel onto Soft Tissues

Besides high adhesion strength, ionogels also demonstrated high burst pressure (Figure 5a). The D_1H_4 ionogel applied onto collagen sheets formed strong bonding *in situ*, and even upon an air pressure of 120 kPa, negligible expansion in the shape of the ionogel occurred, which indicated both high mechanical property and strong adhesion. Burst pressure was inversely proportional to DES amounts in the ionogels (Figure S22), and values for the D_1H_4, D_2H_3, D_3H_2, and D_4H_1 ionogels were 129.0, 73.4, 40.0, and 16.2 kPa, respectively (Figure 5b). Due to enhanced intermolecular interactions and strong hygroscopicity of DES and PDMAPS, the D_1H_4 ionogel showed high burst pressure in water and acidic solutions (Figure S23). Burst pressures of the D_1H_4 ionogel were 103.2, 81.27, 64.83, and

37.53 kPa after being immersed in water for 15, 30, 45, and 60 mins, respectively (Figure 5c). Burst pressure decreased with increased immersion time due to decomposition of the bonding layer and thus resulting in poor mechanical and adhesion properties. Importantly, acidic solutions had a negligible influence on the burst pressure of the D_1H_4 ionogel. Furthermore, D_1H_4 and D_2H_3 ionogels were used to assess the *in vitro* biocompatibility of the novel ionogels. Both fluorescence and bright-field images showed the cell viability of HaCaT cells when being cultured without ionogel, and with D_1H_4 ionogel or D_2H_3 ionogel samples (Figure 5d and S24). Further quantification showed that the cell confluency without ionogel, and with D_1H_4 ionogel or D_2H_3 ionogel samples showed a 300% increase from day 1 to day 3 (Figure 5e). Besides, no significant difference was observed between samples. Indeed, cell metabolic activity without ionogel, and with D_1H_4 ionogel or D_2H_3 ionogel samples increased by 1.9-, 1.8-, and 1.7-fold by day 3 (Figure 5f). Similar *in vitro* biocompatibility results were obtained when the cell insert was used (Figure S25). After day 3, cell metabolic activity increased by 1.8-, 2.1-, and 1.8-fold without ionogel, and with D_1H_4 ionogel or D_2H_3 ionogel samples compared to day 1. Lastly, considering its high mechanical compliance and burst pressure, the D_1H_4 ionogel could be applied to a punctured rabbit stomach and gelled *in situ* to seal the hole (Figure 5g). Initially, water came out from the puncture, but the D_1H_4 ionogel rapidly gelled on the soft tissues of the stomach and sealed the puncture, thus preventing water leakage (Figure 5h). Rabbit intestine was also used to assess the burst pressure of ionogels on tissues. Initially, the intestine with a puncture was leaking upon air inflation. After the ionogel was applied and *in situ* gelled, the intestine showed large expansion, indicating the successful sealing of the puncture (Figure 5i). Burst pressure of the D_1H_4, D_2H_3, D_3H_2, and D_4H_1 ionogels onto the rabbit intestine was 41.77, 27.50, 15.90, and 7.20 kPa, respectively (Figure 5j). Table S1 showed that the ionogel exhibited unparalleled advantages in mechanical stretchability, burst pressure, adhesion strength, and ubiquitous usage in various harsh environments. These results demonstrated the great potential of this ionogel for medical adhesives and other applications.

3. Conclusion

This work demonstrates a new ionogel containing zwitterionic PDMAPS and polarized PHEAA, which is prepared in the DES medium through the one-step photopolymerization. The ionogel exhibits fast gelation and high adhesion in the absence of external pressure due to strong intra- and intermolecular interactions. Strong bonding in harsh environments (e.g., water, acidic and basic solutions, different saline solutions, and brimming surfaces) was achieved by this ionogel. Besides, gelation time and adhesion strength of the ionogel in water and acid did not change significantly, highlighting its widespread usage even underwater. The biocompatible ionogel *in situ* gelled on punctured stomach and intestine tissues could successfully prevent liquid leakage due to the high burst pressure. We envision that this mechanically strong and adhesive ionogel is promising in the field of bioengineering, medical adhesives, soft human-machine interfaces, and flexible electronics.

4. Experimental Section

The Experimental Section is available in the Supporting Information.

Supplementary Material

Refer to Web version on PubMed Central for supplementary material.

Acknowledgments

The authors acknowledge funding from the National Institutes of Health (AR073135, AR074234, UG3TR003148, GM126571, EB023052, GM126831) A*STAR under its 2019 AME IRG & YIRG Grant Calls, A2083c0059.

Data Availability Statement

The data that support the findings of this study are available from the corresponding author upon reasonable request.

References

[1]. Yuk H, Lu B, Zhao X, Chem. Soc. Rev. 2019, 48, 1642. [PubMed: 30474663]

[2]. Liimatainen V, Drotlef D-M, Son D, Sitti M, Adv. Mater. 2020, 32, 2000497.

[3]. Liu X, Zhang Q, Duan L, Gao G, Adv. Funct. Mater. 2019, 29, 1900450.

[4]. Lim C, Hong YJ, Jung J, Shin Y, Sunwoo S-H, Baik S, Park OK, Choi SH, Hyeon T, Kim JH, Lee S, Kim D-H, Sci. Adv. 2021, 7, eabd3716. [PubMed: 33962955]

[5]. Tringides CM, Vachicouras N, Lázaro ID, Wang H, Trouillet A, Seo BR, Artola AE, Fallegger F, Shin Y, Casiraghi C, Kostarelos K, Lacour SP, Mooney DJ, Nat. Nanotechnol. 2021, 16, 1019. [PubMed: 34140673]

[6]. Ge G, Wang Q, Zhang Y-Z, Alshareef HN, Dong X, Adv. Funct. Mater. 2021, 31, 2107437.

[7]. Narayanan A, Dhinojwala A, Joy A, Chem. Soc. Rev. 2021, 50, 13321. [PubMed: 34751690]

[8]. Gan D, Xing W, Jiang L, Fang J, Zhao C, Ren F, Fang L, Wang K, Lu X, Nat. Commun. 2019, 10, 1487. [PubMed: 30940814]

[9]. Li W, Liu X, Deng Z, Chen Y, Yu Q, Tang W, Sun TL, Zhang YS, Yue K, Adv. Mater. 2019, 31, 1904732.

[10]. Fan H, Wang J, Tao Z, Huang J, Rao P, Kurokawa T, Gong JP, Nat. Commun. 2019, 10, 5127. [PubMed: 31719537]

[11]. Li J, Celiz AD, Yang J, Yang Q, Wamala I, Whyte W, Seo BR, Vasilyev NV, Vlassak JJ, Suo Z, Mooney DJ, Science 2017, 357, 378. [PubMed: 28751604]

[12]. Cui C, Liu W, Prog. Polym. Sci. 2021, 116, 101388.

[13]. Yuk H, Zhang T, Lin S, Parada GA, Zhao X, Nat. Mater. 2016, 15, 190. [PubMed: 26552058]

[14]. Gao Y, Chen J, Han X, Pan Y, Wang P, Wang T, Lu T, Adv. Funct. Mater. 2020, 30, 2003207.

[15]. Miao Y, Xu M, Zhang L, Adv. Mater. 2021, 33, 2102308.

[16]. Rapp MV, Maier GP, Dobbs HA, Higdon NJ, Waite JH, Butler A, Israelachvili JN, J. Am. Chem. Soc. 2016, 138, 9013. [PubMed: 27415839]

[17]. Cho H, Wu G, Jolly JC, Fortoul N, He Z, Gao Y, Jagota A, Yang S, Proc. Natl. Acad. Sci. USA 2019, 116, 13774. [PubMed: 31209044]

[18]. Xu L, Gao S, Guo Q, Wang C, Qiao Y, Qiu D, Adv. Mater. 2020, 32, 2004579.

[19]. Zhao Q, Lee DW, Ahn BK, Seo S, Kaufman Y, Israelachvili JN, Waite JH, Nat. Mater. 2016, 15, 407. [PubMed: 26779881]

[20]. Meredith HJ, Jenkins CL, Wilker JJ, Adv. Func. Mater. 2014, 24, 3259.

[21]. Wirthl D, Pichler R, Drack M, Kettlguber G, Moser R, Gerstmayr R, Hartmann F, Bradt E, Kaltseis R, Siket CM, Schausberger SE, Hild S, Bauer S, Kaltenbrunner M, Sci. Adv. 2017, 3, e1700053. [PubMed: 28691092]

[22]. Xie C, Wang X, He H, Ding Y, Lu X, Adv. Funct. Mater. 2020, 30, 1909954.

[23]. Wang Y, Jeon EJ, Lee J, Hwang H, Cho S-W, Lee H, Adv. Mater. 2020, 32, 2002118.

[24]. Liu Y, Wang P, Su X, Xu L, Tian Z, Wang H, Ji G, Huang J, Adv. Mater. 2022, 34, 2108820.
[25]. Zhang J, Chen Z, Zhang Y, Dong S, Chen Y, Zhang S, Adv. Mater. 2021, 33, 2100962.
[26]. Xi S, Tian F, Wei G, He X, Shang Y, Ju Y, Li W, Lu Q, Wang Q, Adv. Mater. 2021, 33, 2103174.
[27]. Liu L, Liu Z, Ren Y, Zou X, Peng W, Li W, Wu Y, Zheng S, Wang X, Yan F, Angew. Chem. Int. Ed. 2021, 60, 8948.
[28]. Yu Z, Wu P, Adv. Mater. 2021, 33, 2008479.
[29]. Xu L, Huang Z, Deng Z, Du Z, Sun TL, Guo Z-H, Yue K, Adv. Mater. 2021, 33, 2105306.
[30]. Wu S, Cai C, Li F, Tan Z, Dong S, Angew. Chem. Int. Ed. 2020, 59, 11871.
[31]. Ge G, Zhang Y-Z, Zhang W, Yuan W, El-Demellawi JK, Zhang P, Di Fabrizio E, Dong X, Alshareef HN, ACS Nano 2021, 15, 2698. [PubMed: 33470788]
[32]. Hua Y, Xia H, Jia L, Zhao J, Zhao D, Yan X, Zhang Y, Tang S, Zhou G, Zhu L, Lin Q, Sci. Adv. 2021, 7, eabg0628.
[33]. Bednarz S, Półćwiartek K, Wityk J, Strachota B, Kredatusová J, Beneš H, Piętak AW, Kowalski G, Eur. Polym. J. 2017, 95, 241.
[34]. Xia Q, Chen C, Yao Y, Li J, He S, Zhou Y, Li T, Pan X, Yao Y, Hu L, Nat. Sustain. 2021, 4, 627.
[35]. Francisco M, Bruinhorst AVD, Kroon MC, Angew. Chem. Int. Ed. 2013, 52, 3074.
[36]. Morales JDM, Narváez EM, Matter 2021, 4, 2141.
[37]. Wu SJ, Yuk H, Wu J, Nabzdyk CS, Zhao X, Adv. Mater. 2021, 33, 2007667.
[38]. Tang S, Zhao Z, Chen J, Yang T, Wang Y, Chen X, Lv M, Yuan WZ, Angew. Chem. Int. Ed. 2022, 134, e202117368.
[39]. Zhang Q, Deng Y-X, Luo H-X, Shi C-Y, Geise GM, Feringa BL, Tian H, Qu D-H, J. Am. Chem. Soc. 2019, 141, 12804. [PubMed: 31348651]
[40]. Liu X, Liu J, Lin S, Zhao X, Mater. Today 2020, 36, 102.
[41]. Ge G, Zhang Y, Shao J, Wang W, Si W, Huang W, Dong X, Adv. Funct. Mater. 2018, 28, 1802576.
[42]. Yuan T, Cui X, Liu X, Qu X, Sun J, Macromolecules 2019, 52, 3141.
[43]. Ge G, Lu Y, Qu X, Zhao W, Ren Y, Wang W, Wang Q, Huang W, Dong X, ACS Nano 2020, 14, 218. [PubMed: 31808670]
[44]. Li C, Liu J, Peng H, Sui Y, Song J, Liu Y, Huang W, Chen X, Shen J, Ling Y, Huang C, Hong Y, Huang W, ACS Nano 2022, 16, 1511. [PubMed: 34908409]
[45]. Ma Z, Yang Z, Gao Q, Bao G, Valiei A, Yang F, Huo R, Wang C, Song G, Ma D, Gao Z, Li J, Sci. Adv., 2021, 7, sciadv.abc3012.
[46]. Hunt PA, Ashworth CR, Matthews RP, Chem. Soc. Rev. 2015, 44, 1257. [PubMed: 25582457]
[47]. Wang X, Wang Z, Qiu J, Angew. Chem. Int. Ed. 2021, 60, 26587.
[48]. Li M, Li W, Guan Q, Dai X, Lv J, Xia Z, Ong W-J, Saiz E, Hou X, ACS Nano 2021, 15, 19194. [PubMed: 34797635]
[49]. Wu X, Guo W, Wang L, Xu Y, Wang Z, Yang Y, Yu L, Huang J, Li Y, Zhang H, Wu Y, Li G, Huang W, Adv. Funct. Mater. 2021, 32, 2110066.
[50]. Huang G, Tang Z, Peng S, Zhang P, Sun T, Wei W, Zeng L, Guo H, Guo H, Meng G, Macromolecules 2021, 55, 156.
[51]. Tan H, Jin D, Sun J, Song J, Lu Y, Yin M, Chen X, Qu X, Liu C, Bioact. Mater. 2021, 6, 905.
[52]. Cui C, Gu R, Wu T, Yuan Z, Fan C, Yao Y, Xu Z, Liu B, Huang J, Liu W, Adv. Funct. Mater. 2021, 32, 2109144.

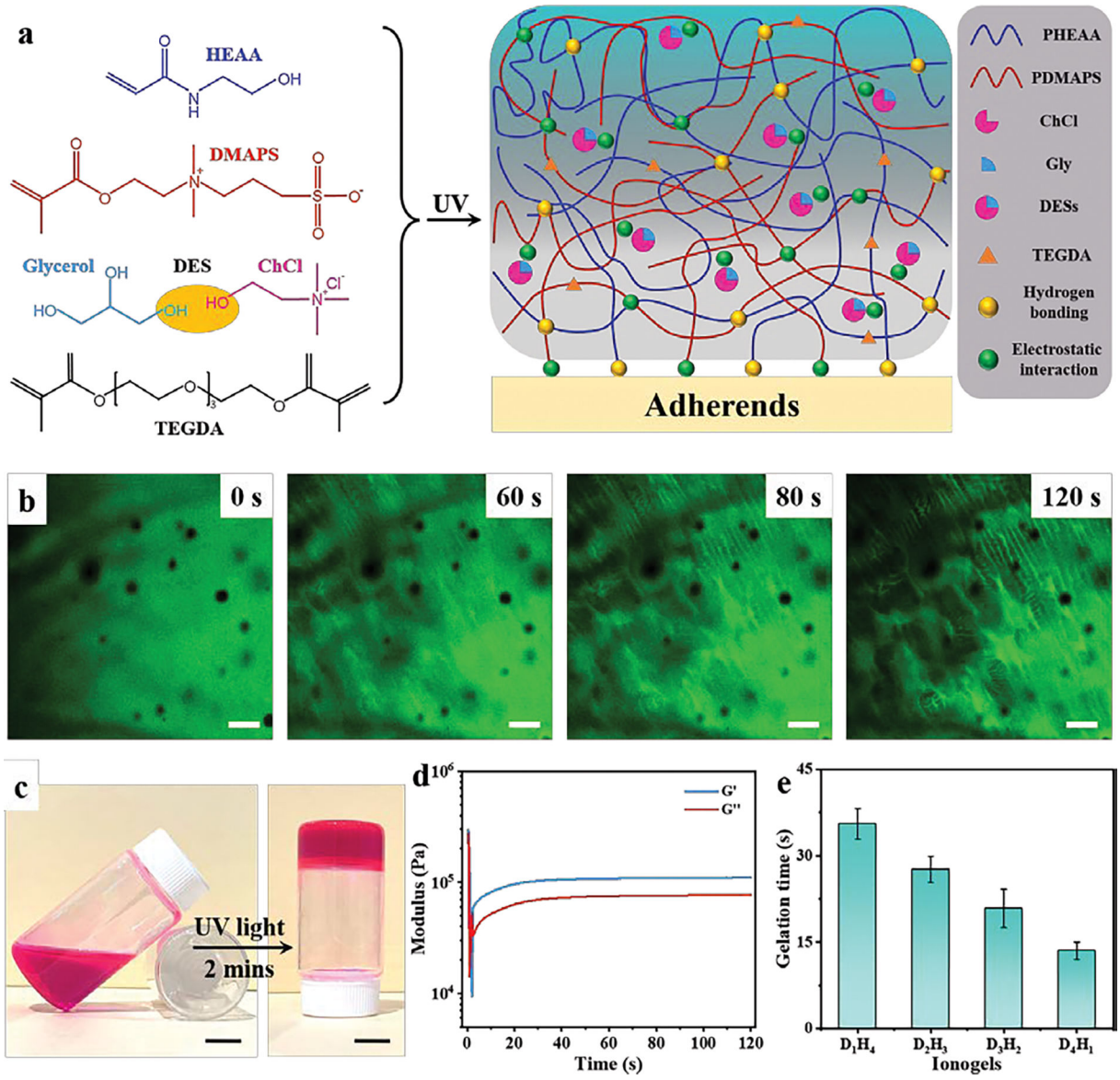

Figure 1.

Characteristics of the rapidly gelled ionogels. (a) Schematic of the adhesive ionogel containing PHEAA, PDMAPS, and DESs. (b) Confocal laser scanning microscopy (CLSM) images show the structural evolution of the D_1H_4 ionogel upon different UV exposure time. Scale bar: 200 μm. (c) Pictures showing the fast gelation feature of the D_1H_4 ionogel upon UV exposure. Scale bar: 1 cm. (d) Modulus variations of the D_1H_4 ionogel during gelation. (e) Gelation time of the D_xH_y ionogels upon UV exposure. The error bars represent standard deviation; sample size n = 3.

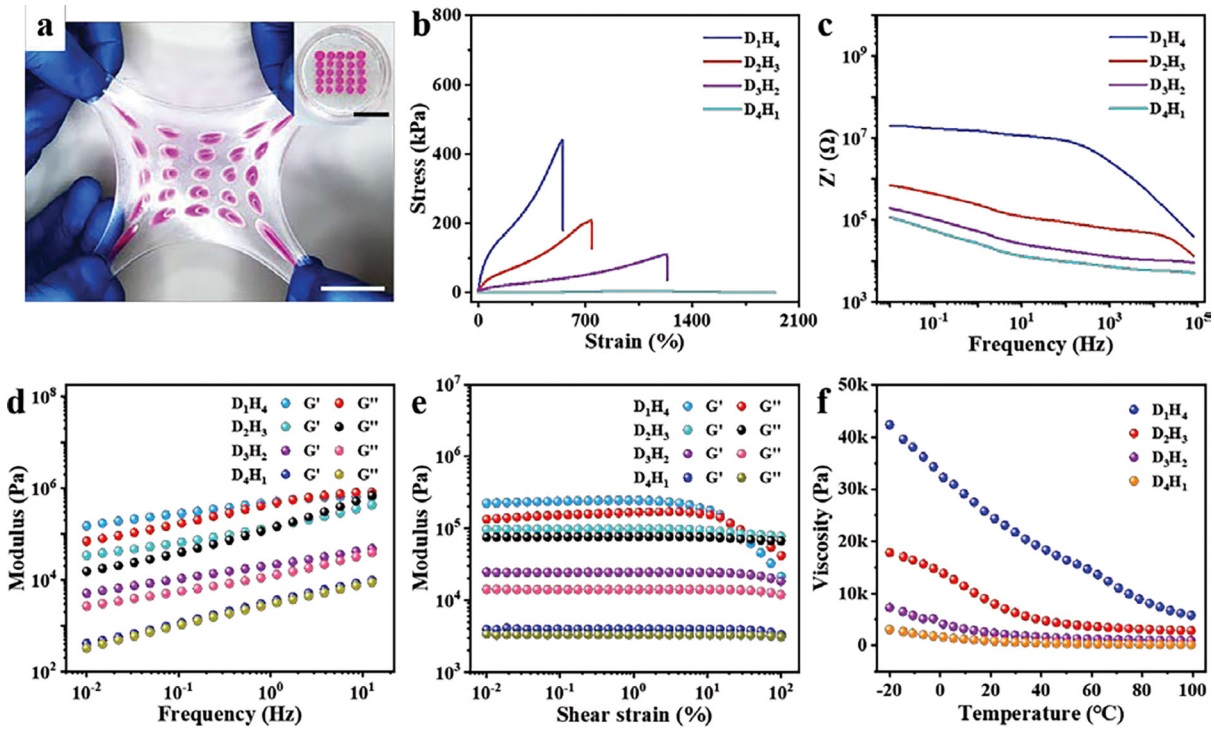

Figure 2.

(a) Illustration of the biaxially stretchable ionogel. Ionogel dots, stained by a pink dye, were dripped and solidified on the transparent bulk ionogel to show the high adhesion between both during biaxial stretching. Scale bar: 2 cm. Inset shows the initial shape of the bulk ionogel dotted with pink ionogel drops. Scale bar: 2 cm. (b) Mechanical and (c) electrochemical performances of the D_xH_y ionogels. (d) Frequency sweep and (e) shear strain sweep of the D_xH_y ionogels. (f) Viscosity variations of the D_xH_y ionogels upon temperature sweep from −20 to 100 °C.

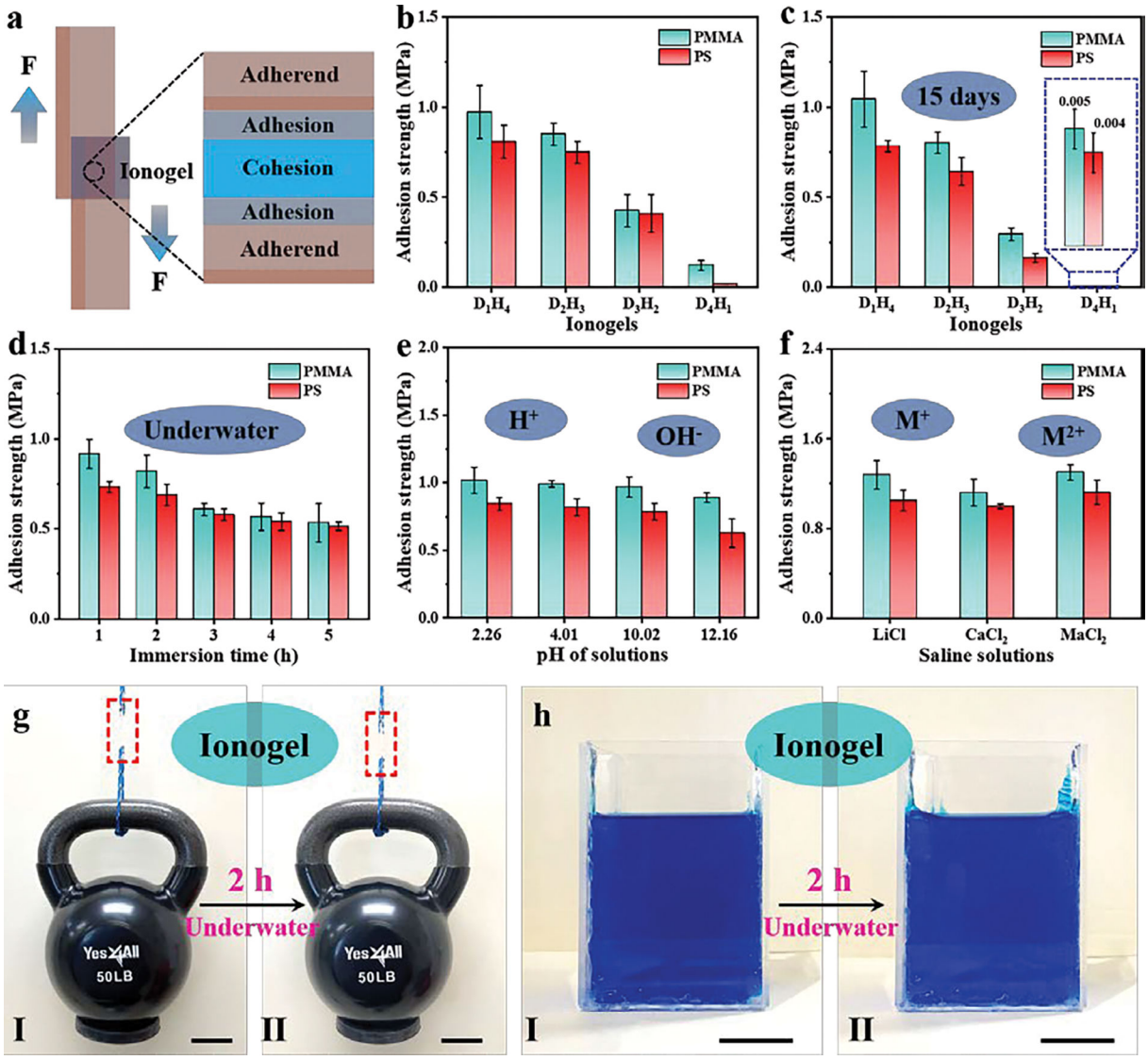

Figure 3.

(a) Schematics of the adhesion mechanism between ionogels and adherends. (b) The adhesion strength of the D_xH_y ionogels onto PMMA and PS adherends. (c) Long-term adhesion of the D_xH_y ionogel. High adhesion of the D_1H_4 ionogel onto PMMA and PS adherends in (d) water, (e) acidic and basic solutions, and (f) different saline solutions (0.5 M) for 2 h. The error bars in Figure 3b–f represent standard deviation; sample size n = 3. (g) The D_1H_4 ionogel bonded between PMMA sheets could lift a 50 lbs kettlebell (Ⅰ) in air and (Ⅱ) after immersion in water for 2 h. Scale bar: 5 cm. (h) The structural integrity of a glass cup made of glass pieces bonded with the ionogel after immersion in water for 2 h. Scale bar: 2 cm.

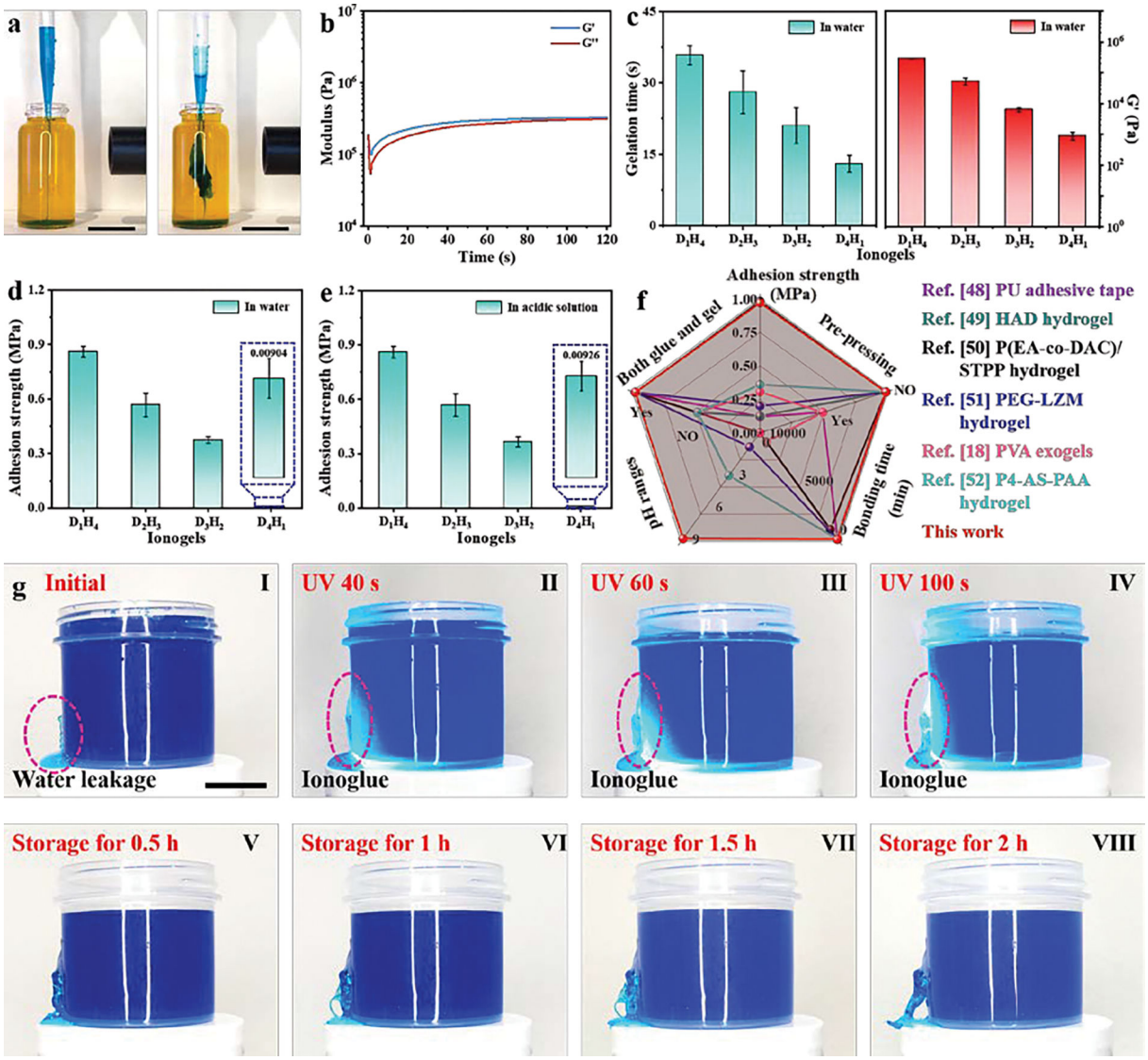

Figure 4.

(a) *In situ* fast gelation of the D_1H_4 ionogel underwater. Scale bar: 2 cm. (b) Modulus variations of the D_1H_4 ionogel during gelation underwater. (c) Gelation time and storage modulus of ionogels gelled underwater. The adhesion strength of the ionogel formed (d) underwater and (e) in acidic solution (pH 1.68). The error bars represent standard deviation; sample size n = 3 in Figure 4c–e. (f) Comparison between the ionogel and recently developed adhesives. (g) Images showing *in situ* fast blocking of water leakage by the D_1H_4 ionogel.

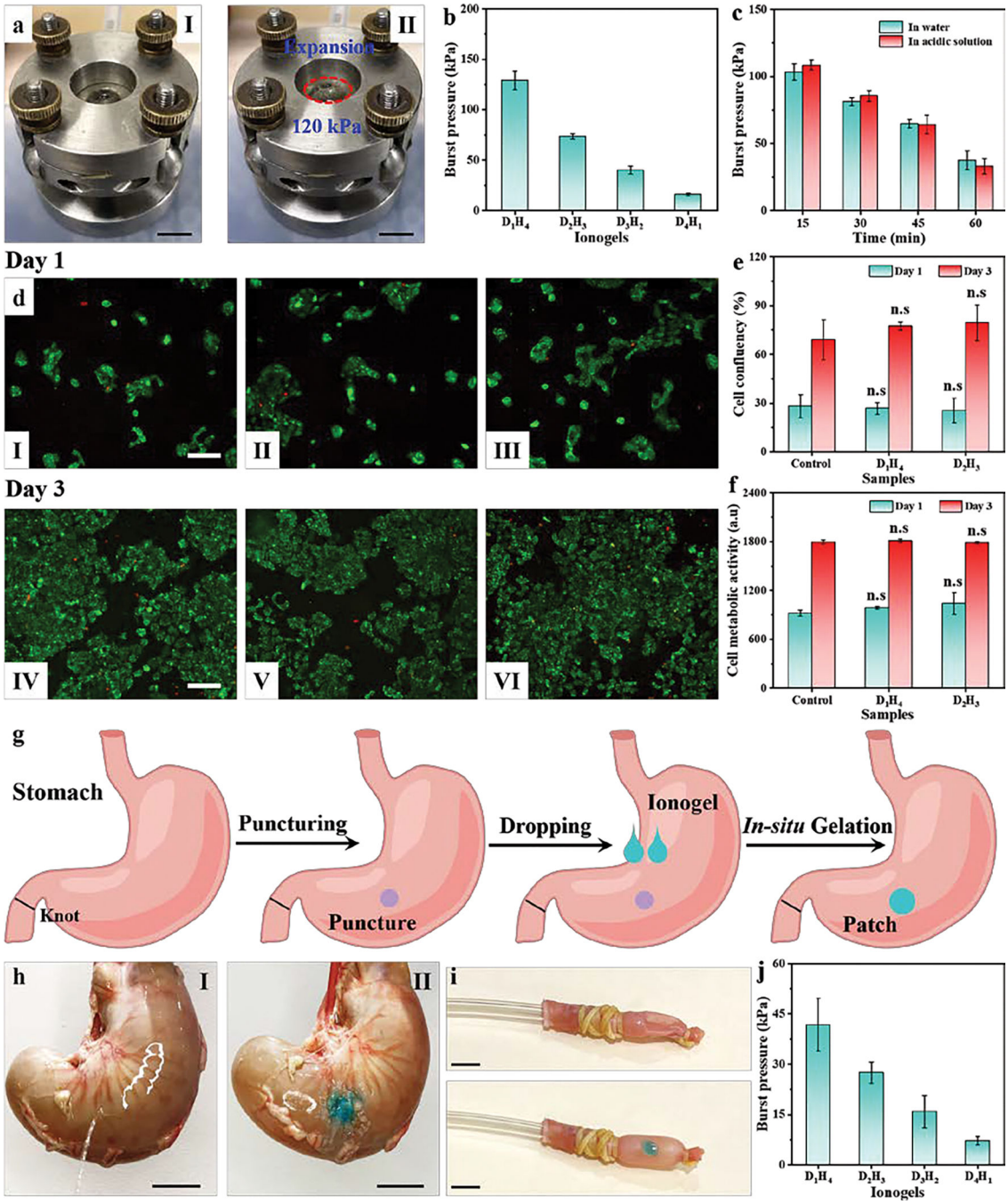

Figure 5.

(a) Images show negligible expansion of the D_1H_4 ionogel after air inflation. Scale bar: 1 cm. (b) Burst pressure of D_xH_y ionogels. (c) Burst pressure of the D_1H_4 ionogel placed in water and acidic solutions (pH 1.68) for a certain time. The error bars represent standard deviation; sample size n = 3 in Figure 5b and c. (d) Fluorescence images of human immortalized keratinocytes (HaCaT) cells without ionogel (Ⅰ and Ⅳ), and with D_1H_4 ionogel (Ⅱ and Ⅴ) or D_2H_3 ionogel (Ⅲ and Ⅵ) samples. Images Ⅰ to Ⅲ referred to day 1, and images Ⅳ to Ⅵ referred to day 3. The green and red colors represent live and

dead cells, respectively. Scale bar: 200 μm. (e) Percentage confluency and (f) cell metabolic activity of HaCaT cells without ionogel, and with D_1H_4 ionogel or D_2H_3 ionogel samples. Student's t-tests were performed for significance test (n.s < 0.01). (g) Schematic showing the *in situ* gelation of the D_1H_4 ionogel onto a punctured rabbit stomach to prevent liquid leakage. (h) Images to show the sealing capacity of the D_1H_4 ionogel to prevent leakage from the stomach. Scale bar: 4 cm. (i) Rabbit intestine with (Ⅰ) puncture and (Ⅱ) the D_1H_4 ionogel onto puncture shows air leakage and an expanded shape upon air inflation, respectively. Scale bar: 0.5 cm. (j) Burst pressure of the D_xH_y ionogels adhered onto rabbit intestines. The error bars represent standard deviation; sample size n = 3 in Figure 5j.